CHEMISTRY
A European Journal

A Journal of
ChemPubSoc Europe

Accepted Article

Title: PAMAM Dendrimers Appended Iron(II)-α-keto Acid Complex on Carbon Nanotubes as Catalytic Nonheme Oxygenase Model

Authors: Debobrata Sheet, Abhijit Bera, Yang Fu, Antonin Desmecht, Olivier Riant, and Sophie Hermans

To be cited as: *Chem. Eur. J.* 10.1002/chem.201901735

Link to VoR: http://dx.doi.org/10.1002/chem.201901735

Supported by
ACES

WILEY-VCH

10.1002/chem.201901735

WILEY-VCH

COMMUNICATION

PAMAM Dendrimers Appended Iron(II)-α-keto Acid Complex on Carbon Nanotubes as Catalytic Nonheme Oxygenase Model

Debobrata Sheet[a][b], Abhijit Bera[c], Yang Fu[a], Antonin Desmecht[a], Olivier Riant*[a], Sophie Hermans*[a]

Abstract: Poly(amidoamine) dendrimers grafted on carbon nanotubes have been appended with iron(II)-α-Keto acid (benzoylformate) complex of polypyridyl ligand to design artificial nonheme oxygenase model. This nano-enzyme was applied for selective catalytic oxidation of organic molecules. While the carbon nanotubes serve as robust heterogeneous platform, the amine-terminals of dendrimers provide catalysts binding sites and the amide-bonds provide a necessary second coordination sphere similar to the enzymatic polypeptide chains. Such hybrid design prevented wrecking down of the primary active sites leading to 8 times faster oxidative decarboxylation rates than its homogeneous analogue. An electrophilic iron(IV)-oxo intermediate has been intercepted that catalyzes the selective oxidation of alcohols to aldehydes and incorporates single oxygen atoms into sulfides and olefins using aerial oxygen with multiple turnover numbers. The catalyst was consecutively regenerated three times by mild chemical treatment and showed negligible loss of activity.

Iron(II) based oxidation catalysts with non-heme ligands have received considerable attention due to their success in catalyzing several challenging C-H bond oxidation reactions.[1] The frontline approaches employ over-stoichiometric amounts of oxidizing agents such as PhIO, H_2O_2, ^tBuOOH etc. to generate iron-oxygen adducts as oxidants, but are often accompanied by highly reactive radicals that lead to non-selective oxidation products.[2] Using enviro-economic dioxygen (O_2) as an alternate oxidant could be an efficient and greener approach but the triplet ground state induces formidable kinetic activation barrier.[3] Metalloenzymes can overcome this barrier using external electron cofactors and can activate dioxygen.[4] Among them, α-Ketoglutarate (α-KG) dependent mononuclear non-heme Fe(II) enzymes are noteworthy and catalyze a myriad of remarkable oxidation reactions in biological processes such as C-H hydroxylation, olefin epoxidation, halogenation, sulfide oxidation etc.[5] These enzymes use an α-keto acid as two-electron sacrificial co-enzyme for the reductive activation of dioxygen. A plethora of molecular functional models built on the understanding of these enzymes have invoked a high valent iron(IV)-oxo intermediate as the plausible oxidant.[2a, 6] However, the practical use of these molecular complexes has not been attained due to the deactivation of the metal-oxygen intermediate through formation of metal bis-μ-oxo complexes or by ligand oxidations.[7] While these dead-end bimolecular reactions and the instability issues can be circumvented by grafting homogeneous complexes on solid supports, the precedents for non-heme iron(II) models are scarce.[8] The proof-of-concept for this approach using non-heme iron(II)-α-Keto acid complex is limited only to one example, where dramatic increase in the reactions rates was registered on immobilizing iron(II)-benzoylformate (BF) complex on alkane-thiolate gold nanoparticles (AuNPs).[9] Recently, iron(II)-benzilate complex on alkane-thiolate AuNPs has shown cis-dihydroxylation reaction of olefins, along with sulfide oxidations. The catalyst however could not be reused due to leaching problems arising from the oxidation of alkane-thiolate chains.[9b] An iron(II)-BPMEN [BPMEN = N_1,N_2-dimethyl-N_1,N_2-bis(pyridin-2-ylmethyl)-ethane-1,2-diamine] complex was immobilized on silica and polymer resin supports. The tethered catalyst demonstrated very modest increase and for some substrates slightly inferior oxidation activity compared to the homogenous analogues.[8d] Thus, despite choosing a robust support, it is essential to provide a secondary protein-like scaffold surrounding the primary active sites to attain synthetic oxygenase catalysts. These components play a crucial role in promoting H-bonding interactions, and modulate steric orientations for optimum interactions among the Fe(IV)-O bonds and the substrates.[10] In this context, carbon nanotubes (CNTs) can be envisaged as a chemically stable and promising nanostructured support with high surface area.[11] They present a well-defined aromatic rings structure that allows covalent and single-site functionalization in a controlled manner. In addition, they are devoid of micropores, as found in activated carbon, which would hinder access to the surface-grafted active sites or limit their possible sizes. In recent years, CNT-dendrimer conjugates have gained limelight as supports, offering higher density of functionalities and improved dispersibility resulting in augmented substrate-catalyst interactions.[12] Additionally, the highly ordered and branched architecture of dendrimers can provide specific conformations where the peripheral functionalities can be appended with catalytically active groups in a precise manner.[13] Among the known dendrimers, the polyamidoamine (PAMAM) dendrimers covalently linked to CNTs can be exploited as a suitable host for active iron(II)-α-keto acid complexes for realizing Fe(II)/O_2 based oxidation catalysts. The amide motifs from PAMAM dendrimer can shape the much needed second coordination sphere, provide secondary interactions and are expected to exert cooperativity effect towards activation of dioxygen. PAMAM dendrimers have been used earlier as a template for several other artificial enzymes.[14]

With these notions in mind, pristine multiwalled carbon nanotubes (*p*-CNTs) were covalently linked with PAMAM dendrimers, the extremities of which were then appended with polypyridyl tripodal ligands (Scheme 1) which were later functionalized with

[a] Dr. D. Sheet, Y. Fu, A. Desmecht, Prof. O. Riant, Prof. S. Hermans, Institute of Condensed Matter and Nanosciences, Molecules, solids and Reactivity (IMCN/MOST)
Universite catholique de Louvain,
Place Louis Pasteur 1, 1348, Louvain-la-Neuve, Belgium
E-mail: sophie.hermans@uclouvain.be, Olivier.riant@uclouvain.be
[b] Dr. D. Sheet
Department of Chemistry, Presidency University, India
Email: debobrata.chem@presiuniv.ac.in
[c] A. Bera
School of Chemical Sciences
Indian Association for the Cultivation of Sciences, India
Supporting information for this article is given via a link at the end of the document.

10.1002/chem.201901735

biomimetic iron(II)-benzoylformate(BF) complex (**4-Fe**) (Scheme 2). The functionalized CNTs were characterized by XPS, ICP, TGA and FTIR. The reactivity of the complex **4-Fe** towards dioxygen and its ability for catalytic oxidation of substrates has been investigated. The catalytic reactivity is also compared with analogous non-immobilized complex (**6-Fe**).

Recently, an efficient protocol towards covalent immobilization of PAMAM dendrimers on CNTs *via* 'grafting to' strategies was established in our lab.[15] Following the same procedure, the amine terminated outer shell of the PAMAM dendrimers **1-G$_0$** (20 wt% in methanol, generation G 0.0) were conveniently converted to azide moieties **[2-G$_0$]** by using Cu(II) catalyst and imidazole-1-sulfonyl azide sulfuric acid salt (Scheme 1).[16] Subsequent reaction with propargyl-functionalized carbon nanotubes (prgCNT) in the same pot resulted in the anchoring of azido-arm of [**2-G$_0$**] onto CNTs through triazole formation to afford **3-G$_0$** (Scheme 1).[15, 17] Sodium ascorbate was used to reduce Cu(II) to Cu(I) to facilitate CuAAC click reaction. The next goal was to attach polypyridyl ligands to the terminals of the grafted dendrimers. For optimizing the conditions for dendrimer functionalization, **2-G$_0$** in soluble form was coupled with four equivalents of alkynyl-polypyridyl (DPAprg) ligand by "click" reaction as well (Scheme S1, ESI). The ESI-MS (in CH_3OH) of the product exhibited a molecular ion peak at *m/z* = 1569.33 attributable to [PAMTrDPA + H^+] (Figure S1a). This peak displayed four units mass shift in CD_3OD indicating the exchange of four triazole protons with the deuterated solvent (Figure S1b). ^{1}H-NMR indicated nearly complete transformation of **2-G$_0$** into triazoles-linked pyridyl ligand (PAMTrDPA) (Figure S2& S3). The *in situ*-formed nanotube-based conjugate [**3-G$_0$**] was then appended with DPAprg ligand by the same click reaction to afford **4-G$_0$** after 48h (Scheme 1).

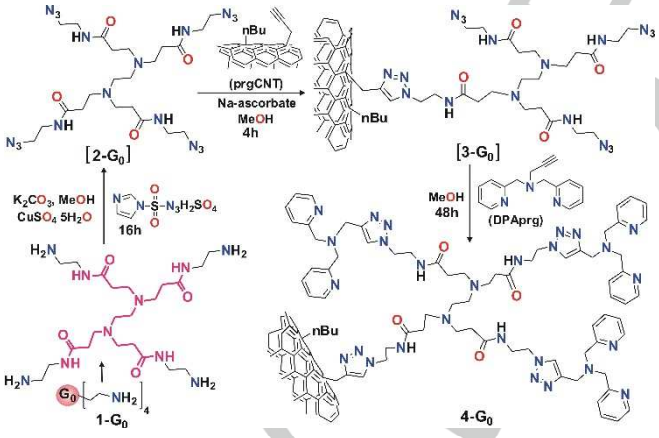

Scheme 1. Synthesis of the functionalized CNTs.

The extent of immobilization of the desired ligands was analyzed by thermogravimetric analysis (TGA) under nitrogen. The isolated conjugate **3-G$_0$** displayed weight loss (18.8%) between 150 ^{0}C to 650 ^{0}C as compared to **prgCNT** (6.8 %) and ***p*-CNT** (0.4%) indicating the decomposition of the dendrimers from CNTs (Figure 1a, 1c, 1e). On formation of **4-G$_0$**, a sharp increase in weight loss to 25.7 % was observed, indicating the decomposition of additional organic moieties apart from dendrimers, which could be attributed to pyridyl ligands (ca. ~0.00018mmole/mg) (Figure 1f). The PAMAM dendrimers can non-covalently wrap around CNTs through charge transfer interactions.[18] It is also established that the covalent immobilization approach affords higher number of grafted dendrimers.[15] Indeed, lower amount of loaded dendrimers (3.8% mass loss) was recorded for the non-covalent conjugate **1-G$_0$(nc)CNT** formed after incubation of **1-G$_0$** with *p*-CNTs for 48h (Figure 1b). The grafting of dendrimers was further confirmed by the appearance of signatures from N1s (6.10 at%) near 399 eV for **3-G$_0$** along with C1s (284.4 eV), and O1s (532.1 eV) in XPS spectrum (Table 1). Higher nitrogen content (9.87 at%) was observed for **4-G$_0$**. The increase in the nitrogen content can be correlated (XPS, $N_{4\text{-}G0}/N_{3\text{-}G0}$ =1.6) to the transformation of three azido-extremities of **3-G$_0$** (total N = 18) to triazoles to form **4-G$_0$** (total N = 27,$N_{4\text{-}G0}/N_{3\text{-}G0}$ =1.5). The non-covalently bound dendrimer **1-G$_0$(nc)CNT** displayed lower content of N(1s) (0.70 at%) reflecting the efficacy of the covalent approach.

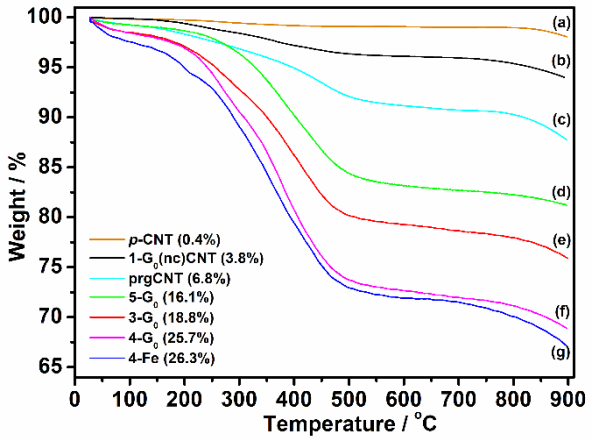

Figure 1. TGA curves for the functionalized CNTs.

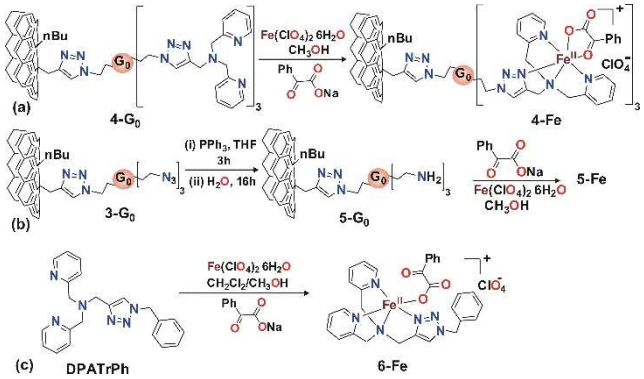

Scheme 2. Synthesis of iron(II) complexes.

The target catalyst **4-Fe** was obtained by the reaction of a methanolic suspension of **4-G$_0$**with [$Fe(ClO_4)_2.6H_2O$] and sodium benzoylformate (NaBF) (Scheme 2a). The XPS survey scan

10.1002/chem.201901735

showed new peaks corresponding to Fe2p (0.92 at%) and Cl2p (0.65 at%). The Fe/N = 0.10 is in close agreement with coordination of iron through pyridyl ligand motif (calculated Fe_3/N_{27} = 0.11) (Figure 2, Table 1). XPS narrow scans for Fe showed a spin-orbit doublet with binding energies of 709.5 and 723.3 eV corresponding to Fe($2p_{3/2}$) and Fe($2p_{1/2}$) respectively (Figure 2 inset). The peak at 709.5 eV is accompanied by a broad shoulder at 713.6 eV attributable to the shake-up satellite due to the high-spin state of iron in the catalyst, which is well expected for such ligand systems.[19] The Cl2p peak was also observed above 207 eV, which could be attributed to the ClO_4^- anions. ICP analysis revealed 1.78 wt% of iron loading. Since the PAMAM dendrimers can themselves coordinate to metal ions through internal N atoms, we synthesized the corresponding Fe(II)/BF complex **5-Fe** from **3-G$_0$** (Scheme 2b). XPS (0.26 at% of Fe, Fe/N = 0.06, expected Fe_3/N_{15} = 0.2) and ICP-AES (0.6 wt%) presented low loading of iron in **5-Fe** (Table 1). The higher Fe content for **4-Fe** thus demonstrates the coordination preference of iron towards pyridyl ligands. Finally, FTIR spectroscopy displayed the characteristic features of the dendrimers grafted onto CNTs along with perchlorate stretching for complex **4-Fe** (Figure S4)[20].

Table 1. XPS data (at.%) of the functionalized CNTs.

Sample	C1s	O1s	N1s	Fe2p	Cl2p	Fe/N
1-G$_0$(nc)CNT	97.25	2.04	0.70	-	-	-
3-G$_0$	84.54	9.36	6.10	-	-	-
4-G$_0$	81.61	8.52	9.87	-	-	-
4-Fe	78.18	11.09	9.16	0.92	0.65	0.10
5-G$_0$	90.42	5.17	4.40	-	-	-
5-Fe	88.29	7.00	4.24	0.26	0.19	0.06

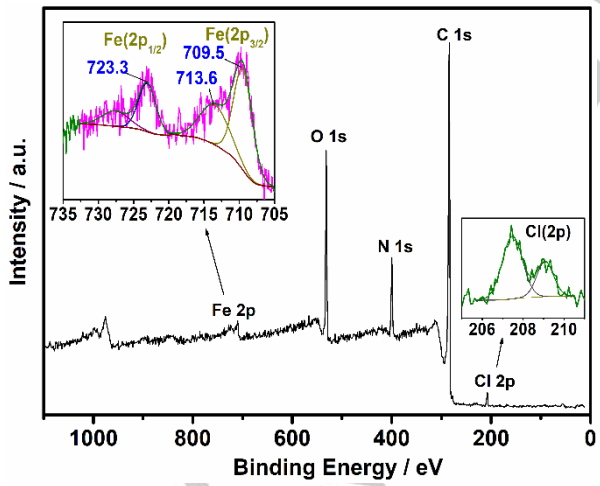

Figure 2. XPS spectra of complex **4-Fe**. Inset: high resolution spectra of Fe2p and Cl2p.

Complex **4-Fe** on reaction with O_2 underwent quantitative decarboxylation of BF to benzoic acid (**4-Fe^{ox}**) only in 6h thereby functionally mimicking the activity of α-Keto acid dependent oxygenase under stoichiometric conditions (Figure S5, Scheme 3). For comparison, the homogeneous iron(II) complex **6-Fe** was also isolated using DPATrPh ligand having 2-pyridyl-1-triazole motif (Scheme 2c&S2, Figure S6).The UV-Vis spectrum showed bands at 317, 370 and 550 nm (Figure S7). The 550 nm band remained intact on reaction with dioxygen. Absence of characteristic charge transfer band (Fe^{II} to π* of the keto group) indicated monodentate coordination of BF to iron in solution.[8] A paramagnetically shifted ^{1}H NMR spectrum was observed for **6-Fe**, indicating the high spin nature of the complex (Figure S8a). As expected, complex **6-Fe** displayed longer reaction time (48h) for the decarboxylation reaction (Figure S9). The dramatic enhancement of decarboxylation rates (8 times) for **4-Fe** was intriguing and can be attributed to the topology of dendrimer branches that exerts cooperative effect, higher dispersions and inhibits dead-end oxo-bridged dimerized or ligand oxidized products. Complex **4-Fe** was reacted with various substrates to intercept any iron-oxygen intermediate (Scheme 3 & Scheme 4)[7b, 21]. With sulfides (100 equiv) as substrates, sulfoxides as a result of oxygen atom transfer reactions (OAT) were selectively formed from the reaction of **4-Fe** with O_2.[7b] For instance, 80% phenyl methyl sulfoxide, and 85% 4-methoxyphenyl methyl sulfoxide were formed from thioanisole and 4-MeO-thioanisolerespectively (Scheme 3, Figure S10& S11, Table S1). The yields represent the interception percentage of the iron-oxygen intermediate formed during the oxidation reaction under stoichiometric conditions. The maximum possible interception will be equal to the benzoate formed from the oxidative decarboxylation of Fe-coordinated BF.[7b] Alcohols such as benzylalcohol selectively formed benzaldehyde (65%), 4-chlorobenzyl alcohol yielded corresponding aldehyde (70%), cinnamyl alcohol afforded cinnamaldehyde (75%) and secondary alcohols such as 1-phenylethanol was oxidized to acetophenone (55%) (Scheme 3, Figure S12-S14). The complex can also carry out epoxidation reactions where cyclooctene was converted to cyclooctane-epoxide (25%). Interestingly, the complex under stoichiometric conditions can activate weak C–H bonds of hydrocarbons and carry out hydrogen atom transfer reactions (HAT). For example, fluorene was converted to fluorenone (23%), dihydroanthracene was converted to anthracene, and 1-adamatanol (16%) was formed from adamantane as substrate (Figures S15-S17).[1d, 5b, 7b] Thus, the synthesized oxygenase model can oxidize a wide array of substrates and is capable of performing both OAT and HAT reactions. Under similar stoichiometric conditions, the oxidant derived from **6-Fe** showed poor substrates interceptions (Scheme 3, Table S1). The *p*-CNTs, and the complex **5-Fe** did not even activate O_2 under these conditions indicating the efficacy of the oxidant derived from complex **4-Fe** in the oxidation reactions.

10.1002/chem.201901735

COMMUNICATION

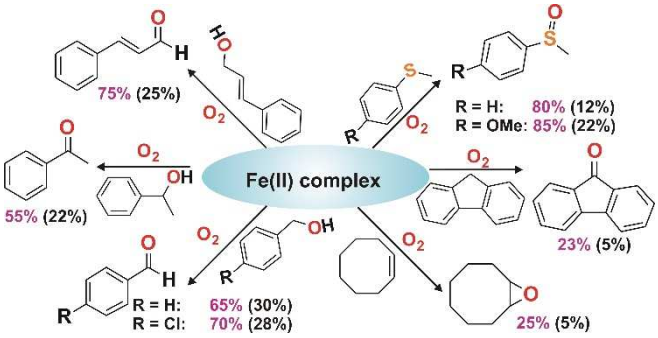

Scheme 3. Substrate oxidation by the Fe(II)-complexes under stoichiometric conditions. Values (in %) indicate the product yields obtained by **4-Fe** (in pink) and **6-Fe** (in brackets).

The reaction of **4-Fe** with thioanisole in the presence of $^{18}O_2$ revealed incorporation of 45% of labelled oxygen atom (^{18}O) in phenyl methyl sulfoxide (Figure S18). A mass shift of two unit from *m/z* = 140 to 142 has been observed. Labelled oxygen atom (^{18}O) was also incorporated in thioanisole oxide (25%) when **4-Fe** was reacted with thioanisole,$^{16}O_2$ and $H_2{}^{18}O$ in acetonitrile solvent (Figure S19). These experiments suggest the formation of an intermediate Fe-O oxidant from aerial oxygen that can exchange O-atom with water.[7b] Hammett analyses with various *para*-substituted thioanisoles revealed a negative ρ value (-0.93), characteristic of an electrophilic oxidant (Figure S20). These results suggest the formation of an iron(IV)-oxo intermediate (**4-Fe^{Im}**) as the oxidant for substrates oxidation (Scheme 4).[1d, 7]

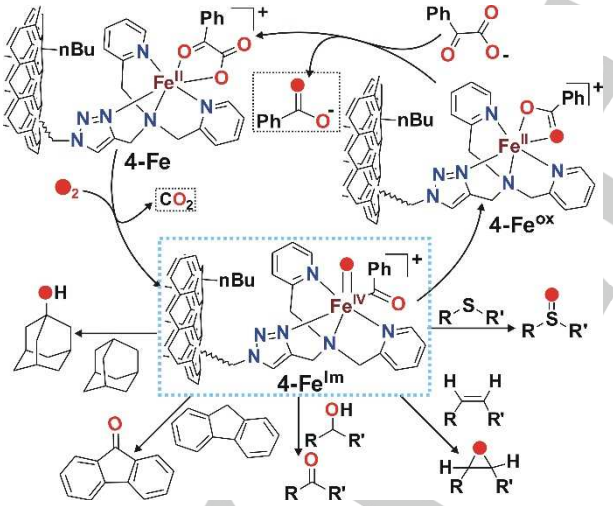

Scheme 4. Mechanism and catalytic oxidation of substrates by complex **4-Fe**.

Our next focus was to investigate the catalytic reactivity of complex **4-Fe** toward alcohols, sulfides and alkenes (Table 2). To facilitate catalytic cycles, excess of BF is added that can displace Fe-coordinated benzoate (**4-Fe^{Ox}**) to regenerate the Fe(II)/α-keto acid complex(**4-Fe)** (Scheme 4). In the case of **4-Fe**, the active site is regenerated following decarboxylation reaction and subsequent generation of the Fe(IV)-oxo oxidant with maximum turnover number (TON_{max} = 11). A TON_{max} of 8 was obtained for oxygen atom transfer (OAT) to sulfides using 4-methylthioanisole and 4-methoxy thioanisole. The yields of epoxides were lower with TON_{max} = 4 for styrene epoxidation reaction. The oxidant from **4-Fe** could selectively transform alcohols to aldehydes with 7 TONs for benzylalcohol substrate. More importantly, the supported catalyst after the first run can be isolated by filtration. The isolated CNTs on treatment with an aq. solution of 1% Na_4EDTA and NH_3 (23%) results in the removal of Fe-ions to regenerate the **4-G$_0$** matrix (Figure S21). The metal ions can also be removed using 2M HCl solution. Further reaction with Fe(II)/NaBF resulted in the reconstruction of the catalyst **4-Fe** (Figure S21). TGA analysis (25 wt% loss), XPS (Fe = 0.84 at%) and ICP (Fe = 2.1 wt%) indicate the regeneration of the catalyst **4-Fe**. The catalyst (**4-Fe$^{[r]}$**) was reused in the same way for three consecutive times. The initial catalytic activity was retained even after 3 cycles (Table 2).

Table 2.Substrate oxidations under catalytic conditions.

Complex	Substrate[a]	Product	TON (S)[b]	TON (BF)[c]
4-Fe	Thioanisole	Thioanisole oxide	6	10
4-Fe	4-Methoxy thioanisole	4-Methoxy thioanisole oxide	8	10
4-Fe	4-Methyl thioanisole	4-Methyl thioanisole oxide	8	11
4-Fe	Cyclooctene	1,2-cyclooctane epoxide	3	10
4-Fe	Styrene	Styrene oxide	4	10
4-Fe	Benzyl alcohol	Benzaldehyde	7	11
4-Fe	Cinnamyl alcohol	Cinnamaldehyde	5	9
4-Fe	1-Phenylethanol	Acetophenone	4	11
4-Fe	4-Chlorobenzyl alcohol	4-Chloro benzaldehyde	6	10
6-Fe	4-Methoxy thioanisole	4-Methoxy thioanisole oxide	0.22	1
6-Fe	Thioanisole	Thioanisole oxide	0.12	1
6-Fe	1-Phenylethanol	Acetophenone	0.23	1
6-Fe	4-Chlorobenzyl alcohol	4-Chloro benzaldehyde	0.28	1
5-Fe	Thioanisole	Thioanisole oxide	0	0
4-Fe$^{[r]}$	Thioanisole	Thioanisole oxide	6	10

[a] Complex: NaBF: Substrate = 1:50:100 equiv. Solvent: 4mL CH_3CN; Time: 8h. [b] TON (substrate oxidation) = mmole of oxidised product/mmole of catalyst. [c] TON (decarboxylation) = mmole of benzoic acid formed/mmole of catalyst. [r] catalysis using regenerated catalyst **4-Fe**(3rd cycle).

Under similar conditions, complex **6-Fe** was dormant towards catalysis (Table 2) and formed Fe(III)-μ-oxo-bridged dimer species as confirmed by ESI-MS and ^{1}H NMR (Figures S8b & S22). Catalytic substrate oxidations using Fe-based models and O_2 are scarce. For instance, a diiron(IV)-μ-oxo oxidant from

Fe(III)-TAML catalyzed oxidation of alcohols.[22] Dioxygen mediated Iron(IV)-oxo from [Fe^{II}(TMC)(CF_3SO_3)$_2$] catalyzed oxidation of sulfides and alcohols with 8 TONs.[23] [(bTAML)Fe^{III}(H_2O)]$^-$ complex showed catalytic TONs up to 80 for olefin epoxidations.[24] Very recently, [($Tp^{PhMe}Fe^{II}$(benzilate)] was found to catalyze C-H bond hydroxylations and *cis*-dihydroxylations with 17 TONs.[24] However, catalytic functional models based on the α-KG dependent nonheme enzymes are limited to [(Tp^{PhMe})Fe^{II}(BF)] (16 TONs) and Fe(II)-BF complex on AuNPs (6 TONs). These models eventually collapse during catalytic cycles.[7b, 9] In contrary, ou r**4-Fe** system can be regenerated repeatedly which increases the overall TONs (>18 for sulfide oxidations), saving time and preparation costs hence making it a superior model ofα-KG dependent non-heme enzymes till date.

In summary, we have developed an efficient protocol for tethering biomimetic polypyridyl ligand-bound Fe(II)-α-Keto acid complex through covalent linkage with PAMAM dendrimers on carbon nanotubes. The PAMAM dendrimers inhibit dead-end bimolecular dimerization, exert cooperative effect, and provide enzymatic shield resulting in dramatic enhancement in activating dioxygen to functionally mimic the activity of α-(KG) dependent non-heme enzymes. An iron(IV)-oxo adduct has been intercepted during the oxidation reaction that could be employed for catalytic selective oxidation of various organic compounds using dioxygen as the oxidant. Furthermore, the catalyst regenerated through mild chemical treatment displayed negligible loss in activity thereby increasing the overall TONs. The current work provides breakthrough approach towards realization of artificial iron(II) based non-heme enzymes as low-cost catalysts for selective aerobic oxidation reactions.

Acknowledgements

The authors wish to thank the Fonds de la Recherche Scientifique (F.R.S.-F.NRS), the Fonds pour la Formation à la Recherche dans l'Industrie et dans l'Agriculture (FRIA), as well as the Universite catholique de Louvain for funding. We are grateful to Jean-Francois Statsyns and Francois Billard for technical assistance. DS is thankful to BELSPO, Belgium for postdoctoral research Fellowship funding. DS is also thankful to Presidency University for FRPDF. AB is thankful to UGC, India for funding. YF is thankful to CSC (China) for his PhD Scholarship.

Keywords: Oxygen activation • nonheme • PAMAM dendrimers • Carbon nanotubes • catalysis

[1] a)C. Gally, B. M. Nestl, B. Hauer, *Angew. Chem., Int. Ed.* **2015**, *54*, 12952-12956; b)K. Suzuki, P. D. Oldenburg, L. Que, Jr., *Angew. Chem., Int. Ed.* **2008**, *47*, 1887-1889; c)C. Zang, Y. Liu, Z.-J. Xu, C.-W. Tse, X. Guan, J. Wei, J.-S. Huang, C.-M. Che, *Angew. Chem., Int. Ed.* **2016**, *55*, 10253-10257; d)A. C. Lindhorst, S. Haslinger, F. E. Kuehn, *Chem. Commun.* **2015**, *51*, 17193-17212; e)S. Jana, M. Ghosh, M. Ambule, S. Sen Gupta, *Org. Lett.* **2017**, *19*, 746-749.

[2] a)W. N. Oloo, L. Que, Jr., *Acc. Chem. Res.* **2015**, *48*, 2612-2621; b)W. Nam, Y.-M. Lee, S. Fukuzumi, *Acc. Chem. Res.* **2014**, *47*, 1146-1154.

[3] a)E. B. Bauer, *Isr. J. Chem.* **2017**, *57*, 1131-1150; b)Y. Liang, J. Wei, X. Qiu, N. Jiao, *Chem. Rev.* **2018**, *118*, 4912-4945; c)K. P. Bryliakov, *Chem. Rev.* **2017**, *117*, 11406-11459; d)H. Sterckx, B. Morel, B. U. Maes, *Angew. Chem., Int. Ed.* **2018**. https://doi.org/10.1002/anie.201804946

[4] a)I. Gamba, Z. Codola, J. Lloret-Fillol, M. Costas, Coord. Chem. Rev. 2017, 334, 2-24; b)L. Que, Jr., W. B. Tolman, *Nature***2008**, *455*, 333-340.

[5] a)R. P. Hausinger, *Crit. Rev. Biochem. Mol. Biol.* **2004**, *39*, 21-68; b)M. Costas, M. P. Mehn, M. P. Jensen, L. Que, *Chem.Rev.***2004**, *104*, 939-986; c)W. Nam, *Acc. Chem. Res.* **2015**, *48*, 2415-2423.

[6] a)S. Martinez, R. P. Hausinger, *J. Biol. Chem.* **2015**, *290*, 20702-20711; b)P. C. A. Bruijnincx, G. van Koten, R. J. M. Klein Gebbink, *Chem. Soc. Rev.* **2008**, *37*, 2716-2744; c)E. I. Solomon, K. M. Light, L. V. Liu, M. Srnec, S. D. Wong, *Acc. Chem. Res.* **2013**, *46*, 2725-2739.

[7] a)Y.-M. Chiou, L. Que, Jr., *J. Am. Chem. Soc.* **1995**, *117*, 3999-4013; b)D. Sheet, T. K. Paine, *Chem. Sci.* **2016**, *7*, 5322-5331; c)T. K. Paine, L. Que, Jr., *Struct. Bonding.* **2014**, *160*, 39-56.

[8] a)S. Fukuzumi, Y.-M. Lee, W. Nam, *ChemCatChem* **2018**, *10*, 1686-1702; b)T. Cheng, Q. Zhao, D. Zhang, G. Liu, *Green Chem.* **2015**, *17*, 2100-2122; c)J. Hong, K. E. Djernes, I. Lee, R. J. Hooley, F. Zaera, *ACS Catal.* **2013**, *3*, 2154-2157; d)Y. Feng, E. G. Moschetta, C. W. Jones, *Chem. - Asian J.* **2014**, *9*, 3142-3152.

[9] a)D. Sheet, P. Halder, T. K. Paine, *Angew. Chem., Int. Ed.* **2013**, *52*, 13314-13318; b) D. Sheet, A. Bera, R. D. Jana, *Inorg. Chem*, **2019**, *58*, 4828-4841.

[10] a)A. S. Borovik, *Acc. Chem. Res.* **2005**, *38*, 54-61; b)O. Cusso, M. W. Giuliano, X. Ribas, S. J. Miller, M. Costas, *Chem. Sci.* **2017**, *8*, 3660-3667; c)R. L. Shook, A. S. Borovik, *Inorg. Chem.* **2010**, *49*, 3646-3660; d)M. Puri, L. Que, Jr., *Acc. Chem. Res.* **2015**, *48*, 2443-2452; e)A. J. Mitchell, N. P. Dunham, R. J. Martinie, J. A. Bergman, C. J. Pollock, K. Hu, B. D. Allen, W.-c. Chang, A. Silakov, J. M. Bollinger, C. Krebs, A. K. Boal, *J. Am. Chem. Soc.* **2017**, *139*, 13830-13836.

[11] a)Y. Yan, J. Miao, Z. Yang, F.-X. Xiao, H. B. Yang, B. Liu, Y. Yang, *Chem. Soc. Rev.* **2015**, *44*, 3295-3346; b)N. Karousis, N. Tagmatarchis, D. Tasis, *Chem. Rev.* **2010**, *110*, 5366-5397; c)A. Hirsch, *Angew. Chem., Int. Ed.* **2002**, *41*, 1853-1859; d)D. S. Su, S. Perathoner, G. Centi, *Chem. Rev.* **2013**, *113*, 5782-5816.

[12] a)M. Shen, X. Shi, *Nanoscale* **2010**, *2*, 1596-1610; b)A.-M. Caminade, J.-P. Majoral, *Chem. Soc. Rev.* **2010**, *39*, 2034-2047; c)F. Giacalone, V. Campisciano, C. Calabrese, V. La Parola, Z. Syrgiannis, M. Prato, M. Gruttadauria, *ACS Nano* **2016**, *10*, 4627-4636.

[13] a)S. M. Grayson, J. M. Frechet, *Chem Rev* **2001**, *101*, 3819-3868; b)S. Campidelli, C. Sooambar, E. Lozano Diz, C. Ehli, D. M. Guldi, M. Prato, *J. Am. Chem. Soc.* **2006**, *128*, 12544-12552; c)T. Palacin, H. L. Khanh, B. Jousselme, P. Jegou, A. Filoramo, C. Ehli, D. M. Guldi, S. Campidelli, *J. Am. Chem. Soc.* **2009**, *131*, 15394-15402.

[14] a)A.-M. Caminade, S. Fruchon, C.-O. Turrin, M. Poupot, A. Ouali, A. Maraval, M. Garzoni, M. Maly, V. Furer, V. Kovalenko, J.-P. Majoral, G. M. Pavan, R. Poupot, *Nat. Commun.* **2015**, *6*, 7722; b)L. Liu, R. Breslow, *J. Am. Chem. Soc.* **2003**, *125*, 12110-12111; c)J. Kofoed, J.-L. Reymond, *Curr. Opin. Chem. Biol.* **2005**, *9*, 656-664.

[15] A. Desmecht, T. Steenhaut, F. Pennetreau, O. Riant, S. Hermans, *Chem-Eur, J.***2018**.*24*, 12992-13001

[16] G. T. Potter, G. C. Jayson, G. J. Miller, J. M. Gardiner, *J. Org. Chem.* **2016**, *81*, 3443-3446.

[17] A. Desmecht, S. Hermans, O. Riant, *ChemistryOpen* **2017**, *6*, 231-235.

[18] V. Vasumathi, D. Pramanik, A. K. Sood, P. K. Maiti, *Soft Matter* **2013**, *9*, 1372-1380.

[19] a)L. Li, A. R. Craze, R. Akiyoshi, A. Tsukiashi, S. Hayami, O. Mustonen, M. M. Bhadbhade, S. Bhattacharyya, C. E. Marjo, Y. Wang, L. F. Lindoy, J. R. Aldrich-Wright, F. Li, *Dalton Trans.* **2018**, *47*, 2543-2548; b)T. Zell, P. Milko, K. L. Fillman, Y. Diskin-Posner, T. Bendikov, M. A. Iron, G. Leitus, Y. Ben-David, M. L. Neidig, D. Milstein, *Chem. - Eur. J.* **2014**, *20*, 4403-4413.

[20] B. Pan, D. Cui, F. Gao, R. He, *Nanotechnology* **2006**, *17*, 2483-2489.

10.1002/chem.201901735

[21] a)D. Sheet, S. Bhattacharya, T. K. Paine, *Chem. Commun.* **2015**, *51*, 7681-7684; b)A. Mukherjee, M. Martinho, E. L. Bominaar, E. Muenck, L. Que, Jr., *Angew. Chem., Int. Ed.* **2009**, *48*, 1780-1783.

[22] A. Ghosh, F. Tiago de Oliveira, T. Yano, T. Nishioka, E. S. Beach, I. Kinoshita, E. Muenck, A. D. Ryabov, C. P. Horwitz, T. J. Collins, *J. Am. Chem. Soc.* **2005**, *127*, 2505-2513.

[23] S. O. Kim, C. V. Sastri, M. S. Seo, J. Kim, W. Nam, *J. Am. Chem. Soc.* **2005**, *127*, 4178-4179.

[24] K. K. Singh, S. Sen Gupta, *Chem. Commun.***2017**, *53*, 5914-5917.

[25] S. Chatterjee, S. Bhattacharya, T. K. Paine, *Inorg. Chem.* **2018**,*57*, 10160-10169

…

10.1002/chem.201901735

WILEY-VCH

Entry for the Table of Contents

COMMUNICATION

Artificial oxygenase designed through decoration of carbon nanotubes with PAMAM dendrimers attached to iron(II)-benzoylformate active sites displayed dramatically enhanced reaction rates compared to homogeneous analogues. An iron(IV)-oxo oxidant was intercepted to catalyse the selective aerobic oxidation of alcohols, olefins, and sulfides thereby representing the best heterogeneous catalytic functional model of α-KG dependent enzymes.

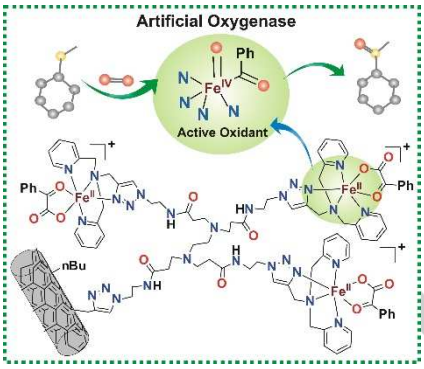

Debobrata Sheet, Abhijit Bera, Yang Fu, Antonin Desmecht, Olivier Riant, Sophie Hermans**

Page No. – Page No.

PAMAM Dendrimers Appended Iron(II)-α-keto Acid Complex on Carbon Nanotubes as Catalytic Nonheme Oxygenase Model